Selective and efficient quantum state tomography and its application to quantum process tomography

Ariel Bendersky[1] and Juan Pablo Paz[2]

[1]*ICFO-Institut de Ciencies Fotoniques, Mediterranean Technology Park, 08860 Castelldefels (Barcelona), Spain*

[2]*Departamento de Física FCEyN UBA and IFIBA CONICET-UBA, Pabellón 1, Ciudad Universitaria, 1428 Buenos Aires, Argentina*

(Received 22 October 2012; published 18 January 2013)

We present a method for quantum state tomography that enables the efficient estimation, with fixed precision, of any of the matrix elements of the density matrix of a state, provided that the states from the basis in which the matrix is written can be efficiently prepared in a controlled manner. Furthermore, we show how this algorithm is well suited for quantum process tomography, enabling one to perform selective and efficient quantum process tomography.

DOI: 10.1103/PhysRevA.87.012122 PACS number(s): 03.65.Wj, 03.67.Pp

I. INTRODUCTION

Quantum information processing tasks always involve the preparation and manipulation of quantum systems. To be able to perform such tasks it is essential to be able to characterize both quantum states and quantum operations. The protocols for characterizing a quantum state are usually referred to as quantum state tomography (QST) [1–6]. In general, QST is a hard task since it involves an exponentially large number of measurements to be preformed (exponentially large on the number of subsystems). Not only that, but the type of measurements that one needs to perform on the systems are usually not easy to perform.

On the other hand, the characterization of quantum processes, known as quantum process tomography (QPT) [1,7–9], is also an exponentially hard task. However, there are some quantum algorithms that allow us to efficiently extract important information about a given quantum process [10–16]. Namely, the partial information obtained by the aforementioned algorithms turns out to be essential for the choice of an error correction algorithm and to compare a given channel with some known target channel. These algorithms do not require performing QST on the final states but measuring quantities such as survival probabilities (or transition probabilities). Other algorithms for QPT, however, do depend upon QST. This makes algorithms for QST an essential tool not just for state tomography, but for process tomography also.

In this paper we will present a method for quantum state tomography. To be specific, it is useful to describe the quantum states in the following way: Let $\mathcal{H}$ be the Hilbert space for the system in question, and let $\mathcal{B} = \{|\psi_a\rangle, a = 1, \ldots, D\}$ be a basis of $\mathcal{H}$, where $D = \dim\mathcal{H}$. Then the density matrix ρ of a state can be written in the basis $\mathcal{B}$ as

$$\rho = \sum_{a,b=1}^{D} \alpha_{ab} |\psi_a\rangle\langle\psi_b|, \tag{1}$$

where $\alpha_{ab} = \langle\psi_a|\rho|\psi_b\rangle$.

In what follows, we will present a method for selective and efficient quantum state tomography (SEQST) that allows one to estimate any coefficient α_{ab} with resources scaling polynomially with the number of subsystems. For this to be possible, we require that any state from the basis $\mathcal{B}$ can be efficiently prepared in a controlled manner. This method, when applied for implementing QPT results in a protocol for efficient and selective QPT that is equivalent to that presented in Refs. [13,14], illustrating one of the virtues of such a selective and efficient QST scheme.

This paper if organized as follows: First we briefly review existing methods for QPT that rely on performing QST in the final states of a certain process. Then we present the selective and efficient algorithm for QST and show how it provides the right tool for efficient and selective QPT, as opposed to previous methods for QST. Finally, we compare that QPT algorithm to that presented in Refs. [13,14], showing how both can be understood in a common theoretical frame.

II. QUANTUM PROCESS TOMOGRAPHY BASED ON STATE TOMOGRAPHY

The goal of QPT is to identify the temporal evolution enforced by a certain quantum process. Any such process is mathematically represented by a linear map $\mathcal{E}$ transforming initial states into final states. In fact, the operation $\mathcal{E}$ is not only linear but also completely positive, and acts as

$$\mathcal{E}(\rho_{\text{in}}) = \rho_{\text{out}}. \tag{2}$$

This operation represents the discrete (input-output) evolution of quantum states. We will focus on maps that are trace preserving and whose output dimension is the same as the input dimension. To describe the quantum map it is convenient to parametrize it in some way. It is simple to notice that any linear map can be written in terms of a certain matrix, known as the χ matrix. This is defined with respect to a certain basis of the space of operators. In fact, if we choose a basis $\{E_m, m = 0, \ldots, D^2 - 1\}$, the χ-matrix representation for $\mathcal{E}$ is determined by the equation

$$\mathcal{E}(\rho) = \sum_{mn} \chi_{mn} E_m \rho E_n^{\dagger}. \tag{3}$$

This description is completely general since the above expressions can be written for any linear channel. Properties of the channel are in one-to-one correspondence with properties of the χ matrix. In fact, the channel preserves the Hermiticity if and only if the χ matrix is Hermitian. Also, the channel preserves trace if and only if the condition $\sum_{mn} \chi_{mn} E_n^{\dagger} E_m = I$ is satisfied. Finally, the channel is completely positive if and only if the χ matrix is positive. Thus, the χ matrix (which,

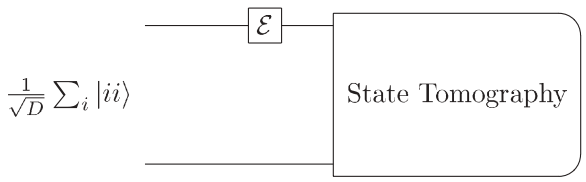

FIG. 1. Scheme for the ancilla assisted process tomography quantum algorithm.

as we mentioned above, depends on the choice of basis for the space of operators) fully describes the channel. Therefore, quantum process tomography is the task of estimating the matrix elements of χ. To achieve this goal there are several methods, some of which involve performing quantum state tomography on final states. Let us review them now.

A. Ancilla assisted quantum process tomography

The ancilla assisted quantum process tomography (AAPT) [7,8] uses n ancillary qubits and allows one to extract all the information about the channel. However, as presented in Refs. [7,8], it only allows one to obtain full information about the process, being unable to obtain only useful partial information about the channel. Thus it is inherently inefficient as full QPT always is.

This is the first of two methods that we will mention here that exploit the state-channel duality given by Choi-Jamiołkowski isomorphism. Such isomorphism establishes a one-to-one relationship between linear operators from $\mathcal{H}\otimes\mathcal{H}$ to $\mathcal{H}\otimes\mathcal{H}$ and completely positive superoperators acting on the space of operators from $\mathcal{H}$ to $\mathcal{H}$. Choi-Jamiołkowski isomorphism establishes a correspondence between states and channels in the following way:

$$\rho_{\mathcal{E}} = \mathcal{E}\otimes\mathbb{I}(|I\rangle\langle I|), \tag{4}$$

where $|I\rangle = \sum_i |ii\rangle/\sqrt{D}$ is the maximally entangled state. After the application of the channel to one of the parts, one can perform state tomography to the state $\rho_{\mathcal{E}}$, obtaining full information about the process $\mathcal{E}$. Figure 1 illustrates this algorithm.

One of the strengths of AAPT is that the initial state can be another state and not necessarily the maximally entangled state. As the number of independent parameters defining the initial state (the Schmidt number) is D^2, such state can always encode the necessary information to define the quantum channel.

This method, besides requiring n ancillary qubits, has the following two troublesome properties: First, it is not clear if the information from the χ matrix can be directly accessed via measurements on the resulting states. Second but related to the previous point, it is not clear how to use QST on the final state to efficiently extract partial and relevant information on the channel. These two issues will be solved in what follows.

B. Direct characterization of quantum dynamics

The direct characterization of quantum dynamics (DQCD) [8,9] is a quantum algorithm similar to that of AAPT in many aspects. It also resorts to n ancillary qubits and relies on the Choi-Jamiołkowski isomorphism. Contrary to the AAPT, on the DCQD the authors explicitly showed a method to efficiently and selectively measure the diagonal coefficients of the χ matrix; however, off-diagonal elements still require one to invert en exponentially large matrix. This makes the method inefficient.

To describe the method let us consider the operator basis consisting of the n-fold tensor product Pauli operators acting on each qubit. We denote these operators as $\{E_m, m = 0,\ldots,D^2-1\}$. In that basis, the channel description is given by

$$\mathcal{E}(\rho) = \sum_{mn} \chi_{mn} E_m \rho E_n^\dagger. \tag{5}$$

In order to perform diagonal tomography, the algorithm proceeds as follows: First, as for the AAPT, we have to generate the state that is isomorphic to the channel

$$\rho_{\mathcal{E}} = \frac{1}{D}\sum_{ijmn} \chi_{mn} E_m |i\rangle\langle j| E_n^\dagger \otimes |i\rangle\langle j|. \tag{6}$$

Now, the probability of measuring the state $\frac{1}{\sqrt{D}}\sum_i |ii\rangle$ on the output is given by

$$\frac{1}{D}\sum_{kl}\langle kk|\rho_{\mathcal{E}}|ll\rangle = \frac{1}{D^2}\sum_{mn}\chi_{mn}\mathrm{Tr}(E_m)\mathrm{Tr}(E_n^\dagger) = \chi_{00}. \tag{7}$$

Thus, we see that the survival probability of the input state directly gives the coefficient χ_{00}. It is easy to show that the very same method can be used to evaluate any diagonal coefficient of the χ matrix. In fact, the probability of obtaining the final state $\frac{1}{\sqrt{D}}\sum_i E_k\otimes\mathbb{I}|ii\rangle$ is nothing but χ_{kk}. As the set

$$\mathcal{R} = \{E_k\otimes\mathbb{I}|I\rangle, k = 0,\ldots,D^2-1\} \tag{8}$$

forms an orthonormal basis of $\mathcal{H}\otimes\mathcal{H}$, a measurement in that basis will suffice for diagonal tomography of the χ matrix.

The main problem arises when off-diagonal tomography is taken into account. The solution presented in Refs. [8,9] is to use a state other than a maximally entangled state. However, it can be shown that, in the most general case, this procedure requires inverting an exponentially large matrix. Again, this makes the method inefficient.

Below, we will introduce a method for QST that provides not only a convenient tool for QST, but also provides the necessary ingredient missing in AAPT and DCQD to obtain an efficient and selective QPT.

III. SELECTIVE AND EFFICIENT QUANTUM STATE TOMOGRAPHY

The standard method for QST was clearly described in Ref. [1]. This method resorts to the description of the state in the Pauli operator basis as

$$\rho = \frac{1}{D}\sum_i \mathrm{Tr}(\rho E_i)E_i, \tag{9}$$

where E_i are the n-fold Pauli operator basis for an n-qubit system. It is straightforward to perform tomography in this basis by just measuring the expectation value of every E_i. Although this method is indeed selective and efficient, it is not well suited for selective and efficient QPT.

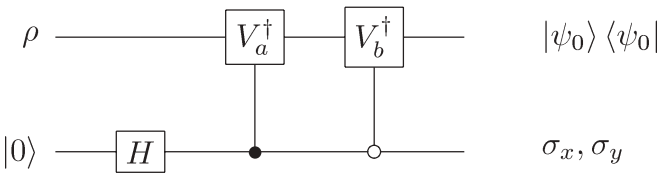

FIG. 2. Quantum circuit for selective and efficient quantum state tomography.

The method we are about to introduce, selective and efficient quantum state tomography (SEQST), is also efficient and selective but, as opposed to the standard method, it is selective in any basis of the corresponding Hilbert space. That is, given the state written in the form

$$\rho = \sum_{a,b=1}^{D} \alpha_{ab} |\psi_a\rangle\langle\psi_b|, \tag{10}$$

and provided we know how to prepare the states from the corresponding basis in a controlled manner, we will be able to selectively measure any given coefficient α_{ab}. Such a measurement will be efficient, meaning that, given a precision, the number of required single-click measurements does not scale with the size of the system.

Consider the circuit shown in Fig. 2 where the operators V_a are the ones that prepare the states from the basis $\mathcal{B} = \{|\psi_a\rangle, a = 1, \ldots, D\}$ from the state $|\psi_0\rangle$ ($V_a|\psi_0\rangle = |\psi_a\rangle$) controlled by the state of the ancilla, and H is a Hadamard gate that acts as $H|0\rangle = \frac{1}{\sqrt{2}}(|0\rangle + |1\rangle)$ and $H|1\rangle = \frac{1}{\sqrt{2}}(|0\rangle - |1\rangle)$. The anticontrolled operation acts whenever there is a $|0\rangle$ on the ancilla and does nothing when the ancilla is on the state $|1\rangle$, as opposed to the controlled operation.

As we will show now, by measuring the average value of the operator $|\psi_0\rangle\langle\psi_0| \otimes \sigma_x$ (that is, the average value of the operator σ_x conditioned on the detection of the state $|\psi_0\rangle$ on the main system) one obtains the real part of χ_{ab}. Moreover, replacing σ_x by σ_y, the same method provides the imaginary part of the same matrix element.

Let us see that. The state corresponding to the system and ancilla that enters the circuit is $\rho_0^{SA} = \rho \otimes |0\rangle\langle 0|$. After applying the Hadamard gate on the ancilla, the resulting state ρ_1^{SA} is given by

$$\begin{aligned}\rho_1^{SA} = {} & \tfrac{1}{2}(\rho \otimes |0\rangle\langle 0| + \rho \otimes |0\rangle\langle 1| \\ & + \rho \otimes |1\rangle\langle 0| + \rho \otimes |1\rangle\langle 1|).\end{aligned} \tag{11}$$

The application of the controlled operations yields the state ρ_2^{SA}:

$$\begin{aligned}\rho_2^{SA} = {} & \tfrac{1}{2}(V_b^\dagger \rho V_b \otimes |0\rangle\langle 0| + V_b^\dagger \rho V_a \otimes |0\rangle\langle 1| \\ & + V_a^\dagger \rho V_b \otimes |1\rangle\langle 0| + V_a^\dagger \rho V_a \otimes |1\rangle\langle 1|).\end{aligned} \tag{12}$$

We will now show how the real part is obtained via measuring $|\psi_0\rangle\langle\psi_0| \otimes \sigma_x$, but the imaginary part is obtained exactly the same way; replacing σ_x by σ_y. That is,

$$\begin{aligned}&\mathrm{Tr}\big(\rho_2^{SA} |\psi_0\rangle\langle\psi_0| \otimes \sigma_x\big) \\ &= \tfrac{1}{2}\langle\psi_0|V_b^\dagger \rho V_a|\psi_0\rangle + \tfrac{1}{2}\langle\psi_0|V_a^\dagger \rho V_b|\psi_0\rangle \\ &= \tfrac{1}{2}(\langle\psi_b|\rho|\psi_a\rangle + \langle\psi_a|\rho|\psi_a\rangle) = \mathrm{Re}\,\alpha_{ab}.\end{aligned} \tag{13}$$

Thus,

$$\mathrm{Tr}\big(\rho_2^{SA} |\psi_0\rangle\langle\psi_0| \otimes \sigma_x\big) = \mathrm{Re}\,\alpha_{ab}, \tag{14}$$

$$\mathrm{Tr}\big(\rho_2^{SA} |\psi_0\rangle\langle\psi_0| \otimes \sigma_y\big) = \mathrm{Im}\,\alpha_{ab}, \tag{15}$$

where the ancilla off-diagonal terms vanish because both σ_x and σ_y have zeros on the diagonal. This is the result we wanted to prove.

To discuss the efficiency of the method we should analyze the resources needed by this algorithm. First of all, the efficiency of the method is limited by that of the implementation of the controlled-$V_a^\dagger$ and controlled-$V_b^\dagger$ operators. In fact, if the implementation of such controlled operations require $O(f(n))$ operations, then the full circuit will also require $O(f(n))$.

Also, if $V_a^\dagger$ and $V_b^\dagger$ are efficiently implementable (and we are not talking here about their controlled versions) for systems of n qubits, then their controlled versions will also be efficiently implementable with a linear overhead. This is due to the fact that efficient implementation of the noncontrolled $V_a^\dagger$ operations means that they can be implemented in $O(\mathrm{poly}(n))$ single- and two-qubit gates and controlled NOT gates. In order to perform a controlled $V_a^\dagger$ we need to replace every single qubit rotation for a controlled qubit rotation, and every controlled NOT for a Toffoli gate, which is nothing but a three-qubit controlled-controlled NOT [1]. The number of operations needed to implement a controlled single-qubit rotation cannot depend on n, because it is always a two-qubit gate. The Toffoli gates, on the other hand, can be implemented with six controlled NOT gates and nine single-qubit gates [17]. Therefore, there is only a linear overhead in implementing the controlled $V_a^\dagger$ operation when the noncontrolled versions have a known implementation.

The other point to determine the efficiency of the method is to determine the number of experimental runs required to obtain the desired result to a given precision ϵ with a probability of success p. To answer that question we just need to consider that each experimental run gives one of three results (+1 corresponding to $|\psi_0\rangle$ on the system and $|0\rangle$ on the ancilla, −1 corresponding to $|\psi_0\rangle$ on the system and $|1\rangle$ on the ancilla, and 0 corresponding to another result on the system). The χ-matrix element is estimated by computing the average value these results after performing a certain number of repetitions M. Each of the results are detected at random with their corresponding probabilities. Therefore, one can use a Chernoff bound to show that to obtain the correct result with uncertainty ϵ and a probability p of success, the number of experimental runs M must be such that

$$M \geqslant \frac{2\ln\left(\frac{2}{p}\right)}{\epsilon^2}, \tag{16}$$

which does not depend on n or D. This implies that the method is efficient.

A. Application to quantum process tomography

In this section we will show how the SEQST algorithm is the right tool to perform selective and efficient QPT when combined with the AAPT method reviewed in Sec. II A.

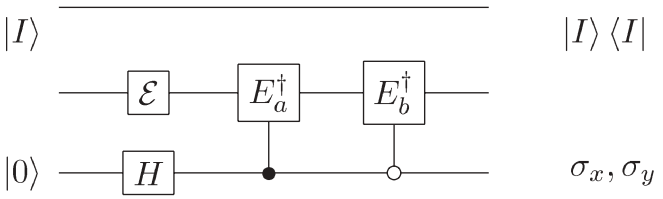

FIG. 3. Application of SEQST to QPT.

In order to proceed, we need to find out the way in which the quantum state isomorphic to the channel $\mathcal{E}$ depends on the χ matrix of such a channel. Thus, we will show that the χ matrix of the channel is nothing but the matrix element of the quantum state in a particular basis. Therefore, by performing quantum state tomography in that basis we directly provide the information about the χ matrix of the channel. To show this, we use Eq. (4) and replace the expansion of $\mathcal{E}$ in the Pauli basis:

$$\rho_{\mathcal{E}} = \sum_{mn} \chi_{mn} E_m \otimes \mathbb{I} |I\rangle\langle I| E_n^\dagger \otimes \mathbb{I}. \tag{17}$$

Indeed, this shows that χ is the matrix representation of $\rho_{\mathcal{E}}$ in the basis $\mathcal{R}$ shown in Eq. (8). Therefore, to selectively measure a single χ coefficient one only needs to perform selective tomography in the basis $\mathcal{R}$.

Using the results already presented in the previous section, we see that to do this we should implement the circuit described in Fig. 3. Here, the application of the channel $\mathcal{E}$ to one of the pieces of the maximally entangled state can be regarded as the preparation of the state isomorphic to the channel. In turn, the rest of the circuit is nothing but the SEQST algorithm described above.

It is important to point out that, since the measurement is direct, the analysis of the resources required to implement the method (presented in the previous section) directly applies to this case. The only extra resources needed in this case are involved in the preparation and measurement of the maximally entangled state which require $O(n)$ additional single- and two-qubit gates.

IV. COMPARISON WITH OTHER SELECTIVE AND EFFICIENT QUANTUM PROCESS TOMOGRAPHY SCHEMES

Another quantum algorithm for selective and efficient quantum process tomography is the one known as SEQPT, precisely for selective and efficient quantum process tomography [13,14]. The main idea there is to follow the procedure described by the circuit shown in Fig. 4 and to estimate the

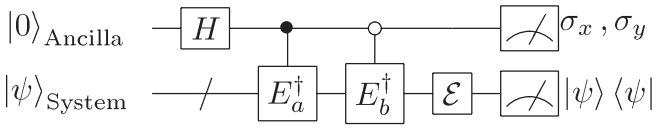

FIG. 4. Circuit for the selective and efficient quantum process tomography algorithm. Depending on the measurement of σ_x or σ_y, the real or imaginary part of χ_{ab} will be obtained.

average answer averaging over the entire Hilbert space of the system using the Haar measure for that purpose. As is shown in Refs. [13,14], that average can be directly related to the matrix element χ_{ab} as

$$\int \langle \sigma_x \otimes |\psi\rangle\langle\psi| \rangle d\psi = \frac{D\text{Re}(\chi_{ab}) + \delta_{ab}}{D+1}, \tag{18}$$

$$\int \langle \sigma_y \otimes |\psi\rangle\langle\psi| \rangle d\psi = \frac{D\text{Im}(\chi_{ab})}{D+1}. \tag{19}$$

Moreover, it can be shown that the average over the entire Hilbert space can be efficiently estimated by randomly sampling over a special (and finite) set of states which is known as a 2-design. For these reasons, the method SEQPT is not only selective but also efficient.

As we mentioned above, in the SEQPT scheme, the average is estimated by randomly sampling states. In the scheme we propose above, the average is obtained *automatically* by the quantum correlation between both parts of the maximally entangled state, without the need to resort to randomly preparing and detecting the special states of the 2-design.

V. SUMMARY

In this paper we presented a quantum algorithm to perform selective and efficient quantum state tomography in any Hilbert space basis, given that the states from that basis can be efficiently prepared in a controlled manner.

We then showed that, when properly combined with the ancilla assisted process tomography, it yields a protocol for QPT that is both selective and efficient. Finally, we showed that this protocol shares some properties with SEQPT, which is a method presented in Refs. [13,14]. The main difference is that the use of ancillae is a way to avoid the preparation of the special states of the 2-design and sampling on them.

ACKNOWLEDGMENTS

This work was partially supported by funds from the CONICET, ANPCyT, UBACyT, EU Q-Essence, and Spanish FIS2010-14830 projects. A.B. is funded by an ERC Starting Grant PERCENT.

[1] M. A. Nielsen and I. L. Chuang, *Quantum Computation and Quantum Information* (Cambridge University Press, Cambridge, UK, 2000).

[2] M. Paris and J. Řeháček, *Quantum State Estimation*, Lecture Notes in Physics (Springer, Berlin, Heidelberg, 2004).

[3] D. Gross, Y.-K. Liu, S. T. Flammia, S. Becker, and J. Eisert, Phys. Rev. Lett. **105**, 150401 (2010).

[4] M. Cramer, M. Plenio, S. Flammia, R. Somma, D. Gross, S. Bartlett, O. Landon-Cardinal, D. Poulin, and Y.-K. Liu, Nat. Commun. **1**, 149 (2010).

[5] C. Miquel, J. P. Paz, M. Saraceno, E. Knill, R. Laflamme, and C. Negrevergne, Nature (London) **418**, 59 (2002).

[6] A. Bendersky, J. P. Paz, and M. T. Cunha, Phys. Rev. Lett. **103**, 040404 (2009).

[7] J. B. Altepeter, D. Branning, E. Jeffrey, T. C. Wei, P. G. Kwiat, R. T. Thew, J. L. O'Brien, M. A. Nielsen, and A. G. White, Phys. Rev. Lett. **90**, 193601 (2003).
[8] M. Mohseni, A. T. Rezakhani, and D. A. Lidar, Phys. Rev. A **77**, 032322 (2008).
[9] M. Mohseni and D. A. Lidar, Phys. Rev. Lett. **97**, 170501 (2006).
[10] J. Emerson, M. Silva, O. Moussa, C. Ryan, M. Laforest, J. Baugh, D. G. Cory, and R. Laflamme, Science **317**, 1893 (2007).
[11] C. C. López, B. Lévi, and D. G. Cory, Phys. Rev. A **79**, 042328 (2009).
[12] B. Lévi, C. C. López, J. Emerson, and D. G. Cory, Phys. Rev. A **75**, 022314 (2007).
[13] A. Bendersky, F. Pastawski, and J. P. Paz, Phys. Rev. Lett. **100**, 190403 (2008).
[14] A. Bendersky, F. Pastawski, and J. P. Paz, Phys. Rev. A **80**, 032116 (2009).
[15] C. T. Schmiegelow, A. Bendersky, M. A. Larotonda, and J. P. Paz, Phys. Rev. Lett. **107**, 100502 (2011).
[16] C. C. López, A. Bendersky, J. P. Paz, and D. G. Cory, Phys. Rev. A **81**, 062113 (2010).
[17] V. V. Shende, and I. L. Markov, Quantum Info. Comput. **9**, 461 (2009).